East Eur. J. Phys. **2**. 115-121 (2021) DOI:10.26565/2312-4334-2021-2-08

PACS: 06.60.Vz, 68.08.De, 68.35.Fx, 81.05.Ni, 81.20.Vj, 81.40.Ef, 81.70.Jb

EFFECT OF Ti, Al, Si ON THE STRUCTURE AND MECHANICAL PROPERTIES OF BORON-RICH Fe–B–C ALLOYS

Olena V. Sukhova
Oles Honchar Dnipro National University
72, Haharin Ave., Dnipro, 49010, Ukraine
Corresponding Author: sukhovaya@ukr.net
Received February 19, 2021; revised March 31, 2021; accepted April XX, 2021

The effects of substitution of Fe in the boron-rich Fe–B–C alloys, containing 10.0–14.0 % B; 0.1–1.2 % C; Fe – the remainder, 5.0 % Ti, Al, or Si (in wt. %) have been studied with optical microscopy, X-ray diffractometry, scanning electron microscopy, energy dispersive spectroscopy. Mechanical properties, such as microhardness and fracture toughness, have been measured by Vickers indenter. The microstructure of the master Fe–B–C alloys cooled at 10 and 10^3 K/s consists of primary dendrites of Fe(B,C) solid solution and Fe_2(B,C) crystals. It has been found that titanium has the lowest solubility in the constituent phases of the Fe–B–C alloys, with preferential solubility observed in the Fe(B,C) dendrites, where Ti occupies Fe positions. This element has been shown to be mainly present in secondary phases identified as TiC precipitates at the Fe_2(B,C) boundaries. Titanium slightly enhances microhardness and lowers fracture toughness of the boron-rich Fe–B–C alloys due to substitutional strengthening of Fe(B,C) dendrites and precipitation of the secondary phases. The level of the content of Al or Si in the Fe(B,C) and Fe_2(B,C) solid solutions and quantity of the secondary phases observed in the structure suggest that more Al or Si are left in the constituent phases as compared with Ti. These elements mainly enter the crystal lattice of Fe_2(B,C) phase replacing iron atoms and form at their boundaries $AlB_{12}C$ and SiC compounds respectively. The additions of Al and Si to the boron-rich Fe–B–C alloys help to modify their fragility: while they slightly decrease microhardness values, addition of these elements improves the fracture toughness of the constituent phases. Increase in a cooling rate from 10 to 10^3 K/s does not bring about any noticeable changes in the solubility behavior of the investigated alloying elements. The rapid cooling gives rise to microhardness and fracture toughness of the phase constituents which average sizes significantly decrease. The effects of the alloying elements on the structure and mechanical properties of the investigated boron-rich Fe–B–C alloys have been explained considering differences in the atomic radii and electronic structure of the solute Ti, Al, or Si atoms.
KEYWORDS: structure, iron borides**,** alloying elements, solubility, microhardness, fracture toughness.

Materials scientists have been striving for several centuries to develop new materials that are stronger, stiffer, and more ductile than existing materials and which can be used at high temperatures [1-3]. It is very important to work out structural materials that require less processing cost and to improve their properties, such as elevated temperature strength and stiffness. Improved properties can ensure higher performance characteristics resulting in extended lifetime [4-6]. The need for these improvements is of particular importance in developing iron alloys [7,8].

The boron-rich Fe–B–C alloys containing more than 10 wt. % B have attracted lots of interest because they can give a challenging opportunity for the potential industrial usage [9,10]. Many investigations have been focused on the solidification behavior of the Fe–B–C alloys [11,12]. These alloys exhibit a broad variety of high physical, chemical, mechanical, and tribological properties [13,14]. Meanwhile, their brittleness retards the development of practical applications. Therefore, boron-rich Fe–B–C alloys have a potential for applications, such as coatings [15,16] or reinforcement particles of composite materials [17,18].

For the use of boron-rich Fe–B–C alloys in many other applications, alloying these alloys with other elements is crucial to achieve the performance specifications that are required. The elements, commonly used for alloying, include titanium, aluminum, silicon etc. [19-23]. But influence of their additions is mainly studied on the Fe–B–C alloys containing up to 3 wt. % B [24-32]. That is why, the research of the effects of alloying by titanium, aluminum, silicon of the boron-rich Fe–B–C alloys produced by the conventional solidification method as well as clarification of their solubility are particularly important for further development of these new materials. Besides, cooling rate during producing alloys also greatly contributes to the solubility of alloying elements in phase constituents thus affecting their properties [33].

Thus, better understanding of the solidification microstructure of the Fe–B–C alloys system with additional elements is essential to support the utilization of these materials. Further work is necessary to understand the solubility behavior of alloying elements in the Fe–B–C alloys and a phase change caused by their addition. Therefore, the purpose of the present work is to investigate the alloying effects of Ti, Al or Si and influence of cooling rate on the structure and mechanical properties of boron-rich Fe–B–C alloys.

MATERIALS AND METHODS

To investigate the structural and mechanical properties of the phases which are present in the cast Fe–B–C alloys cooled at 10 and 10^3 K/s, these alloys were prepared in the following compositional ranges: B (10.0–14.0 wt. %), C (0.1–1.2 wt. %), M (5 wt. %, where M – Ti, Al, or Si), Fe (the remainder). The alloys were prepared by melting of

chemically pure components (<99.99 wt. %) in alumina crucibles in a Tamman furnace. The molten alloys were cooled in the air at the rates of 10 and 10^3 K/s. The chemical analysis was carried out using SPRUT SEF-01-M fluorescent X-ray spectrometer, and each reported value corresponded to the average of three measurements.

To characterize some of structural properties, different analytical techniques were applied. Phase morphology and phase composition were characterized by light-optical microscopy (OM) using NEOPHOT-2 device and JEOL-2010 F scanning electron microscope (SEM) equipped with energy-dispersive spectrometer (EDS). The dendrite parameters of the Fe(B,C) phase, such as a diameter of secondary dendritic arms (d_0) and interdendritic distance (l_0), were measured by quantitative metallography carried out with EPIQUANT image analyzer. The X-ray diffraction (XRD) examination was performed using HZG-4A diffractometer with the Cu-K_α radiation to identify the existing phases of the powdered samples and measure their lattice parameters. For phase identification, measurements were taken for a wide range of diffraction angles ranging from 20° to 120° with a scanning rate of 5 deg/min.

Mechanical properties of the alloys were determined by DURASCAN 20 and PMT-3 Vickers indenters. Vickers microhardness (H_μ) measurements were done by using 0.49 N and 0.98 N loads at room temperature. The loading and unloading times were 10 s each. After the indention, radial cracks appeared from the corner of the indentation along the direction of the diagonal. The fracture toughness (K_{IC}) was evaluated from the crack length initiated at the corners of the Vickers microindentation using an empirical equation proposed in [34]. At least ten indentation tests were made, and the experimental errors were also analyzed.

RESULTS AND DISCUSSION

The major constituents of the master boron-rich Fe–B–C alloys within the investigated concentration range are $Fe_2(B,C)$ and Fe(B,C) solid solutions [12]. The primary solid solution Fe(B,C) arises on the base of iron monoboride and grows in the form of three-dimensional dendrite. Solid solution $Fe_2(B,C)$ is formed afterwards via peritectic reaction $L+Fe(B,C)\rightarrow Fe_2(B,C)$ or crystallizes directly from the liquid because its stoichiometric composition is close to the composition of the peritectic point. The carbon solubility in Fe_2B iron hemiboride measured by EDS is about 1.9 at%. The Fe(B,C) phase has been found to dissolve up to 1.2 at. % of carbon.

When titanium is added to Fe–B–C alloys, it dissolves in the iron borides in small amounts (Table 1) forming preferentially solid solutions with iron monoboride (Fig. 1). Only traces of the element are revealed by EDS as small but noticeable background (Fig. 1b). Consequently, at the $Fe_2(B,C)$ boundaries, the numerous light crystals of TiC secondary phase are seen in the SEM micrographs. The addition of titanium that dissolves in the Fe(B,C) lattice replacing iron atoms causes some distortions due to the difference in atom size (Table 2). Besides, compared with $Fe_2(B,C)$ phase, the increase in microhardness H_μ and the decrease in fracture toughness K_{IC} of Fe(B,C) crystals tend to be more marked (Table 3) while the Fe(B,C) dendrite parameters remain practically unchanged (Table 4).

Table 1. Elemental analysis (in at. %) of the doped Fe–12.1B–0.1C alloys cooled at 10 K/s

Phase	Fe	B	C	Ti	Al	Si	ΣMn,Si,Al,Fe
Fe–12.1B–0.1C–5Ti alloy							
Fe(B,C)	48.0	49.2	0.5	1.1	–	–	1.2
$Fe_2(B,C)$	65.1	31.9	0.8	0.5	–	–	1.7
TiC	–	1.20	49.2	49.3	–	–	0.3
Fe–12.1B–0.1C–5Al alloy							
Fe(B,C)	48.8	48.7	1.1	–	0.5	–	0.9
$Fe_2(B,C)$	61.4	30.8	1.8	–	4.7	–	1.3
$AlB_{12}C$	–	85.5	7.1	–	7.2	–	0.2
Fe–12.1B–0.1C–5Si alloy							
Fe(B,C)	48.6	48.9	0.4	–	–	0.8	1.3
$Fe_2(B,C)$	60.1	31.9	0.9	–	–	5.9	1.2
SiC	–	1.6	49.1	–	–	48.9	0.4

Table 2. The lattice parameters of Fe(B,C) and $Fe_2(B,C)$ crystals in the doped Fe–12.1B–0.1C alloys cooled at 10 K/s

Alloying element	Fe(B,C) (rhombic lattice)			$Fe_2(B,C)$ (tetragonal lattice)		
	a, Å	b, Å	c, Å	a, Å	c, Å	c/a
w/o	5.5051±0.0061	4.0628±0.0097	2.9480±0.0007	5.1130±0.0008	4.2399±0.0035	0.8292
Ti	5.5060±0.0020	4.0642±0.0003	2.9485±0.0011	5.1131±0.0012	4.2400±0.0007	0.8292
Al	5.5057±0.0031	4.0637±0.0019	2.9484±0.0009	5.1171±0.0031	4.2442±0.0015	0.8294
Si	5.5053±0.0012	4.0633±0.0030	2.9481±0.0025	5.1164±0.0007	4.2438±0.0023	0.8295

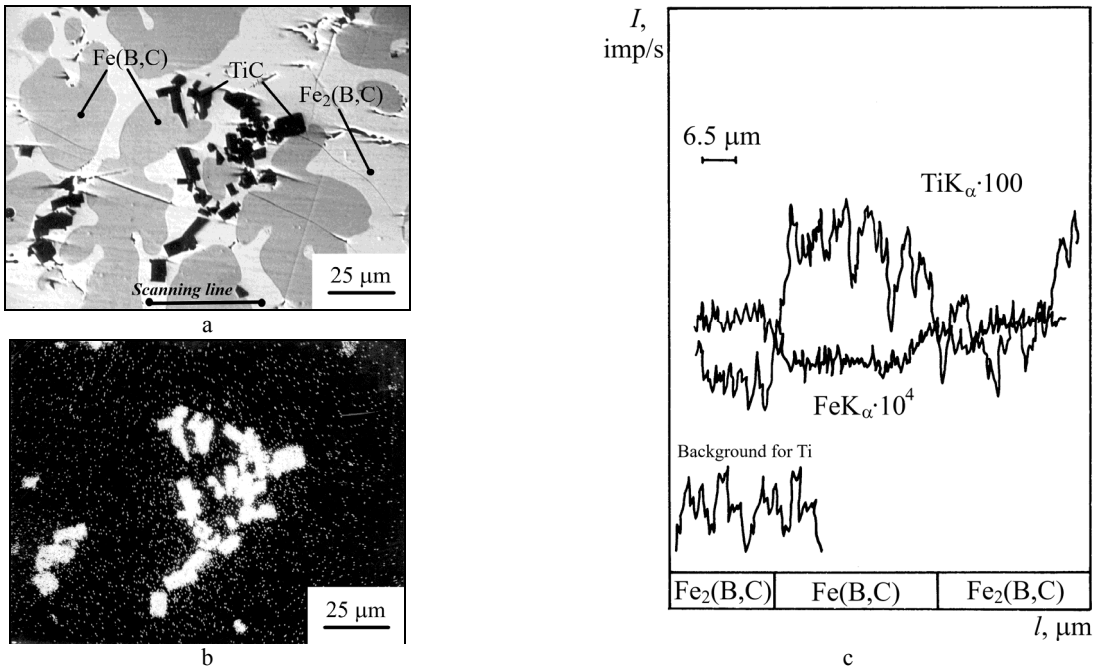

Figure 1. SEM of polished cross-sections of Fe–12.1B–0.1C alloy doped by 5 % of Ti: a – second electron image; b – elemental EDS X-ray mapping in TiK_α radiation; c – elemental profile along scanning line

Table 3. Influence of alloying elements on microhardness (H_μ, GPa) and fracture toughness (K_{1C}, MPa·√м) of $Fe_2(B,C)$ and Fe(B,C) solid solutions

Alloying element	V_{cool}=10 K/s				V_{cool}=10^3 K/s			
	Fe(B,C)		$Fe_2(B,C)$		Fe(B,C)		$Fe_2(B,C)$	
	H_μ	K_{1C}	H_μ	K_{1C}	H_μ	K_{1C}	H_μ	K_{1C}
w/o	17.8±0.3	2.1±0.2	15.8±0.2	2.2±0.3	20.1±0.3	5.0±0.2	17.0±0.1	4.0±0.1
Ti	18.2±0.2	1.8±0.3	16.0±0.3	2.0±0.1	20.5±0.3	4.7±0.1	17.1±0.2	3.2±0.2
Al	17.7±0.1	2.0±0.1	15.2±0.1	3.3±0.2	19.9±0.1	5.3±0.3	15.9±0.3	-
Si	17.7±0.2	2.2±0.2	15.4±0.3	3.0±0.1	20.0±0.2	5.1±0.1	16.2±0.3	-

Table 4. Influence of alloying elements on the interdendritic distance (l_0, μm) and diameter of secondary dendritic arms (d_0, μm) of Fe(B,C) dendrites

Alloying element	V_{cool}=10 K/s		V_{cool}=10^3 K/s	
	d_0	l_0	d_0	l_0
w/o	29.9±0.9	33.1±0.3	4.9±0.2	5.2±0.2
Ti	29.6±0.7	32.9±0.4	4.7±0.1	5.0±0.2
Al	28.7±0.3	32.4±0.2	4.5±0.3	4.8±0.3
Si	29.1±0.5	31.1±0.3	4.6±0.2	4.9±0.1

Unlike titanium, aluminum slightly dissolves in Fe(B,C) dendrites but preferentially – in $Fe_2(B,C)$ crystals (Fig. 2, Table 1) which is in good agreement with XRD measurements of lattice parameters of Fe(B,C) and $Fe_2(B,C)$ phases (Table 2). Besides, with boron and carbon aluminum forms $AlB_{12}C$ secondary phase that precipitates at the boundaries of $Fe_2(B,C)$ crystals (Fig. 2ab). This implies that solid solubility limit is exceeded for 5 % Al. That is why this element is continually pushed out in the melt ahead of the moving solid-liquid interface into the interdendritic regions of growing Fe(B,C) dendrites slowing their growth and causing minor refinement (Table 4). The Fe–B–C alloys with 5 % Al are softer but more ductile (Table 3). So, aluminum, as such, works in the opposite way as that described for titanium.

The additions of silicon to the boron-rich Fe–B–C alloys dissolve in negligible quantities in the dendrites of Fe(B,C) solid solution and enter mainly $Fe_2(B,C)$ phase substituting for the iron atoms (Fig. 3, Table 1, 2). In the SEM micrographs, Fe(B,C) crystals look dark (Fig. 3b). The EDS studies also indicate the formation of light crystals of SiC secondary phase at the $Fe_2(B,C)$ boundaries. This means that a portion of Si becomes incorporated into the solidified phases, but solubility limit forces the remaining solute into the residual liquid after the primary phases have formed. Therefore, alloying with this element slightly decreases dendrite parameters of Fe(B,C) crystals (Table 4). The addition of silicon to the Fe–B–C alloys does not have a substantial effect on the mechanical properties of Fe(B,C) dendrites but decreases microhardness H_μ and increases fracture toughness K_{IC} of $Fe_2(B,C)$ crystals (Table 3).

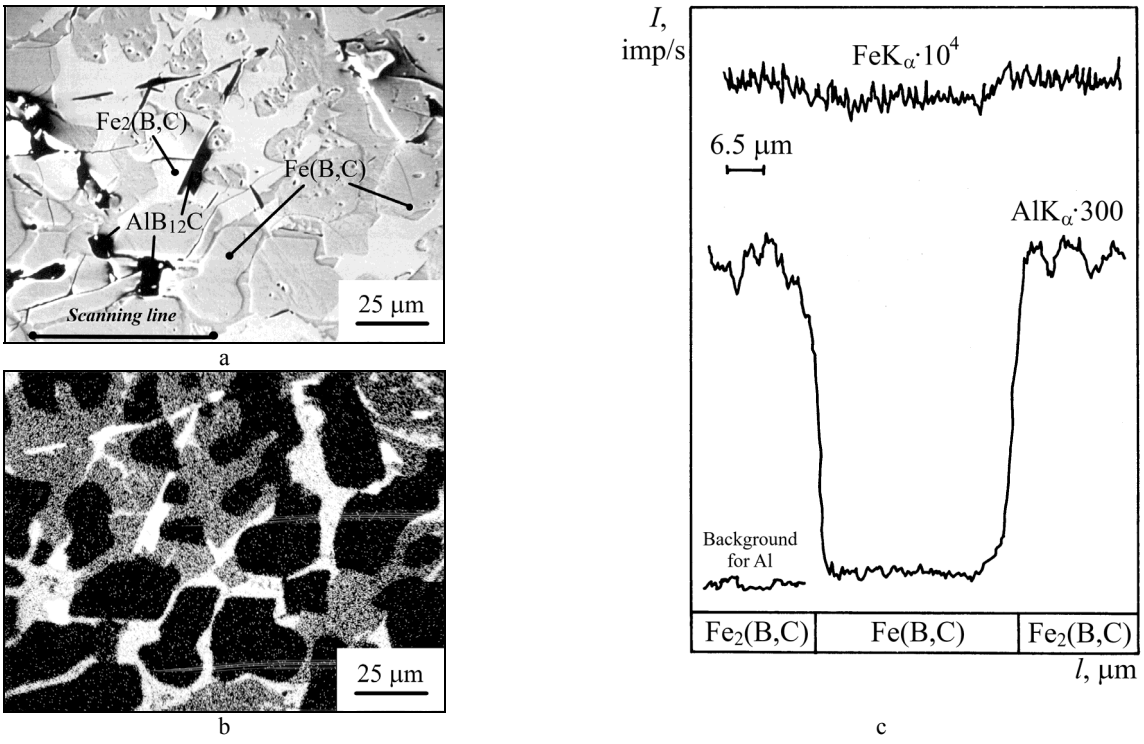

Figure 2. SEM of polished cross-sections of Fe–12.1B–0.1C alloy doped by 5 % of Al: a – second electron image; b – elemental EDS X-ray mapping in AlK_α radiation; c – elemental profile along scanning line

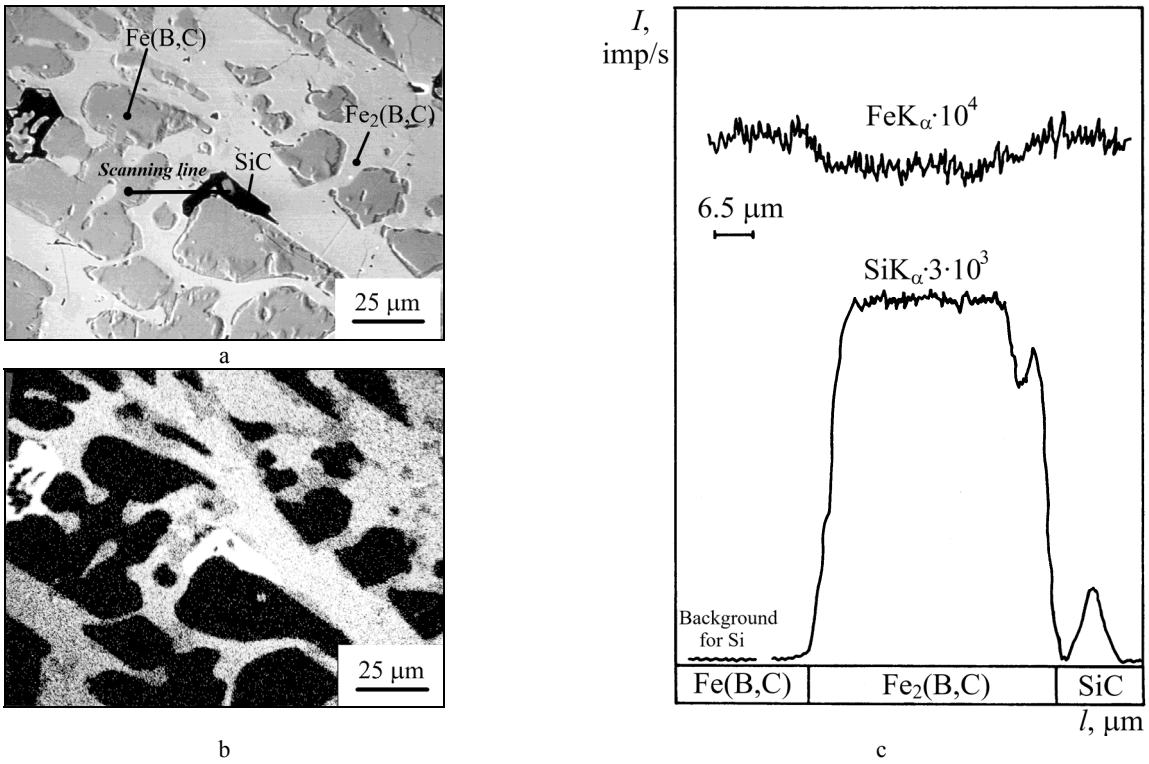

Figure 3. SEM of polished cross-sections of Fe–12.1B–0.1C alloy doped by 5 % of Si: a – second electron image; b – elemental EDS X-ray mapping in SiK_α radiation; c – elemental profile along scanning line

The increase in a cooling rate from 10 to 10^3 K/s does not bring about significant changes in the structural and phase composition of the boron-rich Fe–B–C alloys, saving Fe(B,C) and $Fe_2(B,C)$ crystals become smaller (Table 4). The solubility behavior of Ti, Al, Si in the phase constituents remains unchangeable as the results of the lattice parameters measurements evidence (Table 5). The influence of alloying elements on the mechanical characteristics of the rapidly cooled alloys proves to be similar to that for the alloys cooled at the rate of 10 K/s, with higher cooling rate giving rise to higher H_μ and K_{IC} values (Table 3).

As the obtained results show, the solubility of the investigated alloying elements in the constituent phases of the boron-rich Fe–B–C alloys increases in the following sequence: Ti→Al→Si. Considering the atomic radii of the alloying elements allows to explain their solubility, as in this order the atomic radii decrease [35]. Therefore, the largest distortions are caused by alloying with Ti, and the smallest being caused by alloying with Si, followed by Al. It is also evident why titanium preferentially enters into the less close-packed rhombic lattice of Fe(B,C) dendrites than into the tetragonal lattice of Fe_2(B,C) crystals. Besides, titanium gives the microhardness of Fe(B,C) crystals slight increase caused by substitutional strengthening related to the local distortions caused by the solute atom. This is because the significantly larger atom size of substituting Ti, as compared with that of Fe, interrupts the orderly arrangement of atoms in the iron monoboride lattice.

Table 5. The lattice parameters of Fe(B,C) and Fe_2(B,C) crystals in the doped Fe–12.1B–0.1C alloys cooled at 10^3 K/s

Alloying element	Fe(B,C) (rhombic lattice)			Fe_2(B,C) (tetragonal lattice)		
	a, Å	b, Å	c, Å	a, Å	c, Å	c/a
w/o	5.5041±0.0052	4.0596±0.0106	2.9501±0.0037	5.1120±0.0001	4.2418±0.0011	0.8298
Ti	5.5083±0.0014	4.0640±0.0029	2.9562±0.0025	5.1125±0.0020	4.2416±0.0008	0.8297
Al	5.5055±0.0033	4.0611±0.0016	2.9542±0.0041	5.1172±0.0021	4.2478±0.0040	0.8301
Si	5.5049±0.0010	4.0602±0.0008	2.9607±0.0011	5.1157±0.0004	4.2461±0.0003	0.8300

In assessing the alloying effects, it is also necessary to consider the electronic structure of the constituent phases, including the electron distribution [36]. To the properties of Fe_2(B,C) and Fe(B,C) phases contribute strength and directedness of the bonds connecting atoms in their crystal lattices. The properties of Fe_2B compound are determined by the combination of the covalent Fe−B bonds and metallic Fe−Fe bonds, and those of FeB compound – by the combination of the covalent B−B bonds and metallic Fe−Fe bonds [37]. The strength of these bonds depends on the way in which the bonding electrons are localized. So, when Fe atoms are replaced by atoms of the alloying elements, the relative change in the amount of the collectivized valence electrons forming the atomic bonds is responsible for the observed changes in mechanical properties. In electronic exchange between the atoms of iron and alloying elements, energy gain may be achieved when some valence electrons of iron transfer to the outer shells of the solutes. This means that solutes should preferentially act as electron acceptors.

Considering electronic structure of titanium with incomplete *d*-shell [36], it may be concluded that any re-distribution of bonding electrons caused by replacing iron with titanium in the crystal lattices of Fe(B,C) and Fe_2(B,C) phases leads to the destruction of stable configurations. That is why, titanium negligibly enters the crystal lattices of iron borides. As a result, titanium slightly contributes to the mechanical properties of Fe(B,C) and Fe_2(B,C) phases and may affect the microhardness and fracture toughness of the alloys mainly via the precipitation of TiC secondary phase.

The ions of aluminum and silicon form with boron the similar atomic bonds as the atoms of iron. With their valence electrons, aluminum and silicon can form the bonds either accepting or donating shell electrons. When dissolving, these elements are most likely able to form the metal–metal bonds. This contributes to the limited solubility of these elements in the lattices of iron borides and formation of secondary phases. When Al and Si substitute Fe, the fewer electrons may take part in the electronic exchange [36], which leads to weakening atomic bonds of the Fe_2(B,C) and Fe(B,C) solid solutions. Accordingly, microhardness and brittleness of these structural constituents are found to slightly decrease. Taking into account the limited dissolution of Al and Si as well as their small contribution to the bonds' energy balance, their influence on mechanical properties stands to reason.

CONCLUSIONS

The master boron-rich Fe–B–C alloys were found to consist of two major constituents, namely: Fe(B,C) and Fe_2(B,C) solid solutions. When adding 5 % of Ti to Fe–B–C alloys cooled at 10 K/s, this element has low solubility in the structural constituents, preferentially dissolving in Fe(B,C) phase and forming substitutional solution. The negligible dissolution of titanium in the Fe–B–C alloys is responsible for the appearance of TiC secondary crystals at the Fe_2(B,C) boundaries. The solubility behavior of titanium may be explained by its electronic structure that imposes restrictions on the exchange of valence electrons. Titanium introduces the largest lattice distortions which relates to the relatively large difference in the atomic sizes between the iron and the substituting atom. As a result, the microhardness of Fe(B,C) crystals slightly increases but the fracture toughness decreases.

Aluminum and silicon have a limited solubility in the Fe–B–C alloys dissolving preferentially in Fe_2(B,C) crystals and replacing iron atoms. At that, the minor refinement of structure is observed when Al or Si are added. Al or Si are also found in the form of correspondingly $AlB_{12}C$ and SiC compounds precipitated at the Fe_2(B,C) boundaries. The higher solubility of Al and Si in the boron-rich Fe–B–C alloys, as compared with Ti, may be attributed to the stronger acceptor abilities of these elements. The effects of Al and Si on the mechanical properties of the Fe–B–C alloys may be explained by a local change of the electronic structure of constituent phases which leads to weaker bonded atoms in the crystals. As a result, microhardness and brittleness of Fe(B,C) and Fe_2(B,C) solid solutions slightly decrease.

With cooling rate increasing from 10 to 10^3 K/s, solubility behavior of Ti, Al, Si does not have any noticeable changes. Titanium has negligible dissolution in Fe(B,C) phase forming secondary TiC precipitates but aluminum and

silicon, on the contrary, mainly dissolve in $Fe_2(B,C)$ crystals forming $AlB_{12}C$ and SiC compounds, correspondingly, at the $Fe_2(B,C)$ boundaries due to limited solubility. Cooling rate favors the significant decrease in the dimensions of the constituent phases giving rise to their microhardness and fracture toughness.

The work was performed within the framework of research project No. 0118U003304 "Investigation of the processes of super-rapid quenching from melts and vapor of metal alloys and dielectric compounds" (2018-2020).

ORCID ID

Olena V. Sukhova, https://orcid.org/0000-0001-8002-0906

REFERENCES

[1] V.V. Shyrokov, Kh.B. Vasyliv, Z.A. Duryahina, H.V. Laz'ko, and N.B. Rats'ka, Mater. Sci. **45**(4), 473-480 (2009), https://doi.org/10.1007/s11003-010-9204-5.
[2] S.I. Ryabtsev, V.A. Polonskyy, and O.V. Sukhova, Powder Metall. Met. Ceram. **58**(9-10), 567-575 (2020), https://doi.org/10.1007/s11106-020-00111-2.
[3] O.V. Sukhova, V.A. Polonskyy, and K.V. Ustinova, Mater. Sci. **55**(2), 285-292 (2019), https://doi.org/10.1007/s11003-019-00302-2.
[4] V.G. Efremenko, Yu.G. Chabak, K. Shimizu, A.G. Lekatou, V.I. Zurnadzhy, A.E. Karantzalis, H. Halfa, V.A. Mazur, and B.V. Efremenko, Mater. Des. **126**, 278–290 (2017), https://doi.org/10.1016/j.matdes.2017.04.022.
[5] O.V. Sukhova, V.A. Polonskyy, and K.V. Ustinova, Voprosy Khimii i Khimicheskoi Tekhnologii. **6**(121), 77-83 (2018), https://doi.org/10.32434/0321-4095-2018-121-6-77-83. (in Ukrainian)
[6] O.V. Sukhova, J. Superhard Mater. **35**(5), 277-283 (2013), https://doi.org/10.3103/S106345761305002X.
[7] N. Pavlenko, N. Shcherbovskikh, and Z.A. Duriagina, EPJ Appl. Phys. **58**(1), 10601 (2012), https://doi.org/10.1051/epjap/2012110002.
[8] W. Shenglin, China Weld. **27** (4), 46-51 (2018), https://doi.org/10.12073/j.cw.20180603001.
[9] T. Van Rompaey, K. Hari Kumar, and P. Wollants, J. Alloy Compd. **334**(1-2), 173-181 (2002), https://doi.org/10.1016/s0925-8388(01)01777-7.
[10] S. Rades, A. Kornowski, H. Weller, and B. Albert, Chem. Phys. Chem. **12**(9), 1756-1760 (2011), https://doi.org/10.1002/cphc.201001072.
[11] V. Homolova, L. Ciripova, and A. Vyrostkova, J. Phase Equilibria Diff. **36**(6), 599-605 (2015), https://doi.org/10.1007/s11669-015-0424-0.
[12] O.V. Sukhova, K.V. Ustinova, and Yu.V. Syrovatko, Bull. Dnepropetrovskogo Univ. Fizika. Radioelektronika **21**(2), 76-78 (2013).
[13] J. Lentz, A. Röttger, and W. Theisen, Mater. Charact. **135**, 192-202 (2018), https://doi.org/10.1016/j.matchar.2017.11.012.
[14] J. Zhang, J. Liu, H. Liao, M. Zeng, and S. Ma, J. Mater. Res. Technol. (2019), https://doi.org/10.1016/j.jmrt.2019.09.004.
[15] O.V. Sukhova and Yu.V. Syrovatko, Metallofiz. Noveishie Technol. **33**(Special Issue), 371-378 (2011). (in Russian)
[16] Z.A. Duriagina, M.R. Romanyshyn, V.V. Kulyk, T.M. Kovbasiuk, A.M. Trostianchyn, and I.A. Lemishka, J. Achiev. Mater. Manuf. **100**(2), 49-57 (2020), https://doi.org/10.5604/01.3001.0014.3344.
[17] O.V. Sukhova, Metallofiz. Noveishie Technol. **31**(7), 1001-1012 (2009). (in Ukrainian)
[18] I.M. Spiridonova, O.V. Sukhova, and A.P. Vashchenko, Metallofiz. Noveishie Technol. **21**(2), 122-125 (1999).
[19] Z. Chen, S. Miao, L. Kong, X. Wei, F. Zhang, and H. Yu, Mater. **13**(4), 975 (2020), https://doi.org/0.3390/ma13040975.
[20] L. Rovatti, J.N. Lemke, A. Emami, O. Stejskal, and M. Vedani, J. Mater. Eng. Perform. **24**, 4755-4763 (2015), https://doi.org/10.1007/s11665-015-1798-1.
[21] J. Miettinen, V.-V. Visuri, and T. Fabritius, Arch. Metall. Mater. **66**(1), 297-304 (2021), https://doi.org/10.24425/amm.2021.134787.
[22] X. Ren, H. Fu, J. Xing, Y. Yang, and S. Tang, J. Mater. Res. **32**(16), 304-314 (2017), https://doi.org/10.1557/jmr.2017.304.
[23] O. Kon and U. Sen, Acta Phys. Pol. A **127**(4), 1214-1217 (2015), https://doi.org/10.12693/APhysPolA.127.1214.
[24] P. Sang, H. Fu, Y. Qu, C. Wang, and Y. Lei, Materwiss. Werksttech. **46**(9), 962-969 (2015) https://doi.org/10.1002/mawe.201500397.
[25] M.I. Pashechko, K. Dziedzic, and M. Barszcz, Adv. Sci. Technol. Res. **10**(31), 194-198 (2016), https://doi.org/10.12913/22998624/64020.
[26] V.V. Yemets, M.M. Dron`, and O.S. Kositsyna, J. Chem. Technol. **27**(1), 58-64 (2019), https://doi.org/10.15421/081906.
[27] S. Ma and J. Zhang, Rev. Adv. Mater. Sci. **44**, 54-62 (2016).
[28] Z.F. Huang, J.D. Xing, S.Q. Ma, Y.M. Gao, M. Zheng, and L.Q. Sun, Key Eng. Mater. **732**, 59-68 (2017), https://doi.org/https://doi.org/10.4028/www.scientific. net/kem.732.59.
[29] T.N. Baker, Ironmak. Steelmak. **46**(1), 1-55 (2019), https://doi.org/10.1080/03019233.2018.1446496.
[30] A. Sudo, T. Nishi, N. Shirasu, M. Takano, and M. Kurata, J. Nuclear Sci. Technol. **52**(10), 1308-1312 (2015), https://doi.org/10.1080/ 00223131.2015.1016465.
[31] L. Sidney, *Alloy Steel: Property and Use*, (Scitus Academics LLC, Wilmington, 2016).
[32] X. Huang, W.G. Ischak, H. Fukuyama, T. Fujisawa, and C. Yamauchi, ISIJ Int. **36**(9), 1151–1156 (1996), https://doi.org/10.2355/isijinternational.36.1151.
[33] O.V. Sukhova and K.V. Ustinova, Funct. Mater. **26**(3), 495-506 (2019), https://doi.org/10.15407/fm26.03.495.
[34] K. Niihara, R. Morena, and P.H. Hasselman, J. Mater. Sci. Lett. **1**, 13-16 (1982), https://doi.org/10.1007/BF00724706.
[35] C.J. Smithells, *Metals Reference Book*, (Butterworth and Co., London, Boston, 1976).
[36] G.V. Samsonov, I.F. Pryadko, L.F. Pryadko, *Электронная локализация в твердом теле* [*Electron Localization in Solids*], (Nauka, Moscow, 1976), pp. 339. (in Russian)
[37] G. Li and D. Wang, J. Condens. Matter. Phys. **1**, 1799-1808 (1989), https://doi.org/10.1088/0953-8984/1/10/002.

ВПЛИВ Ti, Al, Si НА СТРУКТУРУ ТА МЕХАНІЧНІ ВЛАСТИВОСТІ ВИСОКОБОРИСТИХ СПЛАВІВ Fe–B–C

Олена В. Сухова

Дніпровський національний університет імені Олеся Гончара

49010, Україна, м. Дніпро, просп. Гагаріна, 72

Досліджено вплив заміщення Fe у високобористих сплавах Fe–B–C, що містять 10,0–14,0 % B; 0,1–1,2 % C; Fe – залишок, 5,0 % Ti, Al чи Si (у ваг. %) із застосуванням методів оптичної мікроскопії, рентгеноструктурного аналізу, сканувальної електронної мікроскопії та рентгеноспектрального мікроаналізу. Механічні властивості, а саме мікротвердість та коефіцієнт тріщиностійкості, вимірювали на приладі Віккерса. Мікроструктура базових сплавів Fe–B–C, охолоджених зі швидкістю 10 та 10^3 K/c, складається з первинних дендритів твердого розчину Fe(B,C) та кристалів Fe_2(B,C). Встановлено, що титан має найнижчу розчинність у структурних складових сплавів Fe–B–C, причому Ti переважно розчиняється в решітці фази Fe(B,C), займаючи в ній позиції Fe. Показано, що цей елемент, в основному, бере участь в утворенні вторинних фаз, ідентифікованих як TiC, які спостерігаються в структурі у вигляді виділень по границям фази Fe_2(B,C). Титан незначно підвищує мікротвердість і знижує коефіцієнт тріщиностійкості високобористих сплавів Fe–B–C завдяки твердо-розчинному зміцненню дендритів Fe(B,C) та виділенню вторинних фаз. Розчинність Al та Si в фазах Fe(B,C) та Fe_2(B,C), а також кількість вторинних фаз, що утворюються в структурі, свідчать про більшу розчинність Al та Si у структурних складових порівняно з Ti. Ці елементи переважно розчиняються в кристалічній решітці фази Fe_2(B,C), заміщуючи атоми заліза, а також утворюють по її границях сполуки $AlB_{12}C$ та SiC відповідно. Додавання Al та Si до високобористих сплавів Fe–B–C незначно зменшує мікротвердість і збільшує коефіцієнт тріщиностійкості структурних складових. Підвищення швидкості охолодження з 10 до 10^3 K/c не викликає суттєвої зміни характеру розчинності досліджених легуючих елементів у високобористих сплавах Fe–B–C. Охолодження з більшою швидкістю забезпечує зростання мікротвердості та коефіцієнта тріщиностійкості структурних складових, середні розміри яких стають значно меншими. Вплив легуючих елементів на структуру та механічні властивості досліджених високобористих сплавів Fe–B–C пояснено різницею атомних радіусів та електронної структури розчинених атомів Ti, Al, Si.

КЛЮЧОВІ СЛОВА: структура, бориди заліза**,** легуючі елементи, розчинність, мікротвердість, коефіцієнт тріщиностійкості.